



GPU Nuclear Corporation  
Post Office Box 480  
Route 441 South  
Middletown, Pennsylvania 17057-0191  
717 944-7621  
TELEX 84-2386  
Writer's Direct Dial Number:

(717) 948-8461

4410-87-L-0068  
Document ID 0183P

May 21, 1987

US Nuclear Regulatory Commission  
Attn: Document Control Desk  
Washington, DC 20555

Dear Sirs:

Three Mile Island Nuclear Station, Unit 2 (TMI-2)  
Operating License No. DPR-73  
Docket No. 50-320  
Reactor Pressure Vessel Integrity

GPU Nuclear letter 4410-87-L-0013, dated January 19, 1987, advised that Babcock and Wilcox (B&W), the TMI-2 reactor designer, had been requested to conduct a review of the dose rate profiles obtained from the cavity underneath the Reactor Vessel (RV). Those dose rate profiles were reported in Reference 1.

B&W has concluded their review and provided the results of their analysis (Reference 2). A copy is attached for your information. The analysis concludes that the dose rate profiles measured in March 1986 with miniature ion chambers can be correlated to calculations which assumed cesium contamination sources without assuming there is fuel beneath the RV. The contamination sources considered include the bathtub ring on the Reactor Building (RB) basement wall, RB wall contamination, RV insulation contamination, dissolved activity in basement water, and contamination on pipe surfaces.

Consistent, with the findings of the Burns and Roe (B&R) analysis, the B&W analysis concludes that the correlation of dose rate profiles and assumed contamination sources does not provide conclusive evidence as to the presence or absence of fuel below the RV. In that regard, GPU Nuclear wishes to reiterate that the preponderance of the evidence provides no basis to doubt the integrity of the lower head. Thus, GPU Nuclear plans to continue defueling activities.

8706010124 870521  
PDR ADOCK 05000320  
P PDR

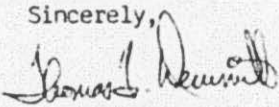
a subsidiary of the General Public Utilities Corporation

A001  
111

May 21, 1987  
4410-87-L-0068

As noted in our letter of January 19, 1987, GPU Nuclear plans to perform a gamma spectrometer survey of the cavity under the RV, as recommended by B&R, as part of the fuel accountability effort on a "non-interfering basis" with defueling. Those survey results will be provided to you as they become available.

Sincerely,



*for* F. R. Standerfer  
Director, TMI-2

FRS/JJB/eml

Attachments

cc: Regional Administrator, Region 1 - W. T. Russell  
Director, TMI-2 Cleanup Project Directorate - Dr. W. D. Travers  
President, Burns and Roe Company - W. R. Cobean

REFERENCES

1. TMI-2 Technical Bulletin 86-25 dated May 2, 1986, Revision 0, "Gamma Scanning of the Cavity Under the Reactor Vessel."
2. "Babcock and Wilcox Analysis of Dose Rate Under TMI-2 Reactor Vessel," Prepared by N. L. Snidow and S. O. King, dated April 13, 1987, B&W Document No. 51-1167938-00.





**Babcock & Wilcox**  
a McDermott company

## ENGINEERING INFORMATION RECORD

Document Identifier 51— 1167938-00

Title Analysis of Dose Rate Under TMI-2 Reactor Vessel

**PREPARED BY:**

Name N. L. Snidow and S. Q. King

Signature *N. L. Snidow* Date 4/13/87  
*S. Q. King* 4/13/87

**REVIEWED BY:**

Name Donald A. Nitti

Signature *Donald A. Nitti* Date 4/13/87

Technical Manager Statement: Initials *JAL*

Reviewer is Independent.

**Remarks:**

This document provides an analysis of the M-7 and M-9 gamma profiles measured with a miniature ion chamber under the TMI-2 reactor vessel in March of 1986. The measured profiles were adequately matched with calculations using reasonable assumptions regarding cesium contamination source strength based on contamination information available from other locations in the basement.

2706010133 870521  
PDR ADOCK 05000320  
P PDR

## CONTENTS

	Page
1. INTRODUCTION . . . . .	5
2. SUMMARY OF RESULTS . . . . .	6
3. MEASUREMENTS . . . . .	7
4. QADMOD CALCULATIONS . . . . .	9
4.1. Case 1 -- Source in Ring on Wall . . . . .	10
4.2. Case 2 -- Source on Wall Below Ring . . . . .	11
4.3. Cases 3, 4, and 5 -- Source on Insulation . . . . .	11
4.4. Cases 6, 7, and 8 -- Source in Water . . . . .	12
4.5. Case 9 -- Localized Source on Guide Pipe . . . . .	12
4.6. Cases 10 and 11 -- Uniform Source on Nozzle and Guide Pipe . . . . .	13
4.7. Case 12 -- 4-Inch High Ring Source on Wall . . . . .	13
5. TRANSPORT CALCULATIONS . . . . .	14
6. RESULTS . . . . .	16
7. REFERENCES . . . . .	17

List of Tables

Table	Page
1. List of QADMOD Cases . . . . .	18
2. Calculated Dose Rate Along M-7 Withdrawal Path . . . . .	19
3. Attenuation in Nozzle and Guide Pipe From QADMOD . . . . .	20
4. Dose Rate From Localized Source on Guide Pipe . . . . .	20
5. Ion Chamber Sensitivity and Guide Pipe Attenuation From DOT Results . . . . .	21

List of Figures

Figure	Page
1. Calculated and Measured Dose Rate, M-7 Traverse . . .	22
2. Primary Shield Cavity Under RPV, Plan View . . . . .	23
3. Primary Shield Cavity Under Reactor Vessel, Elevation View . . . . .	24
4. Path of Incore Guide Pipe #13 . . . . .	25
5. Current Profile Measured at Location M-7 . . . . .	26
6. Path of Incore Guide Pipe #16 . . . . .	27
7. Current Profile Measured at Location M-9 . . . . .	28
8. QADMOD Model for Case 1, Ring Source . . . . .	29
9. Dose Rate From Various Sources, M-7 Traverse . . . . .	30
10. Dose Rate From Localized Source on Guide Pipe . . . . .	31
11. DOT Model . . . . .	32
12. Calculated Ion Chamber Current With Source on Insulation . . . . .	33
13. Calculated Ion Chamber Current With Source in Water . . . . .	34

## 1. INTRODUCTION

Gamma radiation measurements below the TMI-2 reactor vessel were made in March 1986 in an attempt to characterize the gamma radiation present in this region. The measurements were made using a miniature ion chamber inserted into the calibration tube of incore instrument assemblies. The measurements are reported in Reference 1 and include a scan at position M-7 from a reference plane tangent to the bottom of the reactor vessel out to approximately 168 inches withdrawn and a scan at position M-9 from approximately 103 inches withdrawn from the reference plane to about 230 inches withdrawn. Since the measurements were made, there have been several analyses<sup>1,2,3</sup> which have attempted to explain the general shape and magnitude of the measured results as well as the peak that occurred in the M-7 profile near the air/water interface. The primary question is whether the measured results can be reasonably explained without assuming that there is fuel debris outside the reactor vessel.

In the work reported here, calculations were made to provide an independent assessment of these ion chamber measurements. This study addresses the question of whether the ion chamber profiles can be explained based on the cesium contamination known to be in the containment without assuming that there is fuel outside the reactor vessel, thus demonstrating that the profiles by themselves do not prove that there is fuel outside the reactor vessel. It is emphasized that this study cannot prove that there is no fuel in the cavity beneath the reactor vessel. The available ion chamber measurements do not provide sufficient information to reach such a unique conclusion.

The cesium/barium gamma sources considered as contributors to the dose rate beneath the reactor vessel included contamination in a high water level ring on the cavity wall, on the remainder of the wall, on the mirror insulation across the bottom of the reactor vessel, dissolved in the water, and on the surface of the nozzle and guide pipe.

The dose rate beneath the reactor vessel resulting from the various sources was calculated using QADMOD-G, a three-dimensional point kernel gamma shielding code. The response of the ion chamber near the air/water interface was studied with the one-dimensional transport code ANISN and the two-dimensional transport code DOT.

## 2. SUMMARY OF RESULTS

The results are summarized in Figure 1. The curve in the figure is the calculated dose rate for the M-7 traverse due to  $^{137}\text{Cs}$  contamination beneath the reactor vessel. The measured points are from Reference 1 with the exception that the dose rates underwater were converted from the current measurements using an underwater calibration constant determined from the DOT calculation in Section 5. The  $^{137}\text{Cs}$  source strengths, used in the calculations leading to Figure 1, were selected to be in a range considered reasonable based on contamination information available from other locations in the basement and to match the measured data. The agreement between the calculated curve and the measured points in Figure 1 is not to be interpreted as proof that the assumed cesium source strengths are correct; but rather, that it is possible to match the measured data with reasonable assumptions regarding the cesium contamination source strengths without resorting to the assumption that there is fuel beneath the reactor vessel.

The calculated values for the M-7 traverse should also apply to the M-9 traverse over the range of 104 to 165 inches withdrawn. The M-9 measured dose rate is approximately 4.0 R/hr in this range using the underwater calibration constant from DOT. Comparing this with the calculated dose rate in Figure 1 shows that the calculated value is approximately equal to the average of the measured dose rates for M-7 and M-9 in the range of 105 to 165 inches withdrawn.

### 3. MEASUREMENTS

The miniature ion chamber measurements made beneath the TMI-2 reactor vessel in March of 1986 are reported in Reference 1. Five figures from that report are reproduced here as Figures 3 through 7. Figures 3, 4, and 6 describe the geometry of the cavity beneath the reactor vessel and give the location of the incore instrumentation guide pipes for the M-7 and M-9 locations. An incore detector assembly (as shown in Figure 2) is located inside each guide pipe and consists of an outer Inconel wall, an inner Inconel calibration tube, and nine lead wires with  $Al_2O_3$  insulation and Inconel sheaths located in the annular ring between the wall and the calibration tube.<sup>4</sup> A radial traverse from the center of a calibration tube through a lead wire to the outside of the incore assembly passes through 0.057-inch of metal. For calculational purposes, the wall thickness of the nozzle and guide pipes were increased by 0.057-inch to simulate the effect of the incore detector assembly on the ion chamber current.

The gamma measurements were made with a miniature ion chamber having an 0.072-inch OD and a sensitive length of 1.67 inches.<sup>4</sup> The detector had a stainless steel case and was filled with 10 atmospheres of xenon. The measurements were made by inserting the ion chamber to various depths in the center calibration tube of an incore detector assembly and recording the current at each position. Position steps of 6 inches were used for the M-7 traverse and both 1- and 6-inch steps were used for the M-9 traverse. Figures 5 and 7 show the measured ion chamber current for the M-7 and M-9 traverses. Both of these figures are from Reference 1.

The gamma sensitivity of the miniature ion chamber was measured at B&W's Lynchburg Research Center. A value of  $3.47 \times 10^{-13}$  amp/R/hr was determined as the sensitivity in air.<sup>4</sup> The measurement used a collimated  $^{137}Cs$  source with the ion chamber in a mockup of the steel incore nozzle located at the bottom of the reactor vessel. Air filled the space between the source and nozzle. In another measurement, a spent fuel assembly with a cooling time of 14 months was used as the source. The measurement was made underwater 3 feet from the source and yielded a value of  $34.8 \times 10^{-13}$  amp/R/hr.<sup>4</sup> The measured current was converted to dose rate in R/hr in Reference 1 by dividing by the ion chamber sensitivity. The measured sensitivity in air was used for the M-7 data above the air/water interface and the measured sensitivity in water was used for both the underwater M-7 data and for all of the M-9 data.

It was observed in Reference 3 that the measured underwater sensitivity was not appropriate for the specific case encountered here since the source was not distributed in the water. A calibration constant appropriate for the detector in a guide pipe

#### 4. QADMOD CALCULATIONS

QADMOD-G is a three-dimensional point kernel gamma shielding code available from the Radiation Shielding Information Center at ORNL. The code was designed to accommodate complex source geometry configurations and to provide convenient methods of describing shielding and detector locations. A distributed source in the code is represented by a number of point sources (up to 27,000). The distance traveled in a straight line through each region from each point source to each detector position is determined. The uncollided flux and resulting dose rate at each detector point is then determined for each energy group from the attenuation coefficient in each region and the distance traveled in that region. Dose rate from scattered gammas is included through a calculated energy dependent buildup factor which is applied to the direct dose rate. The dose rate at a point is then determined by summing over the energy groups and source points.

QADMOD calculations were made for the 12 cases listed in Table 1 and are documented in Reference 5. The fuel inside the reactor vessel and  $^{137}\text{Cs}$  contamination on surfaces beneath the reactor vessel were considered as sources. Calculations in Reference 2 demonstrated that fuel inside the reactor vessel contributes very little to the total dose rate beneath the reactor vessel. This is due to a combination of low source strength and shielding by the reactor vessel. This result will be used in this study since, even if there is a contribution to the dose rate below the reactor vessel, it only makes it easier to explain the remaining observed dose rate with cesium contamination. That is, any relatively small contribution from the fuel inside the reactor vessel would reduce the assumed contamination on the insulation and perhaps other surfaces beneath the reactor vessel. The calculations, listed in Table 1 were made to determine the dose rate from  $^{137}\text{Cs}$  contamination. The cases include:

- o A "bathtub ring" on the upper part of the cavity wall,
- o The rest of the wall below the ring,
- o The mirror insulation below the reactor vessel,
- o The 2 feet of water in the cavity,
- o Surface of the nozzle and guide pipe,
- o Localized heavier layer on the guide pipe.

The source strength used in each case is largely arbitrary. The calculated dose rate is proportional to the source strength used, therefore, the QADMOD results may be used for any source strength by simply multiplying by a constant. Calculated dose rates are

underwater with a dissolved source is determined in the DOT calculations reported in Section 5 and was used in this report to convert current to dose rate for the underwater data.

required at points along the M-7 withdrawal path as are calculated in Cases 1, 2, 3, and 5. Detector locations along the withdrawal path can be readily modeled in QADMOD, however, a cylindrical guide pipe following the withdrawal path cannot. The guide pipe and nozzle were omitted from Cases 1, 2, 3, and 5. A section of a vertical nozzle and guide pipe was added along the axis for Cases 4 and 7. Cases 5 and 8 are identical to Cases 4 and 7 except the nozzle and guide pipe were omitted in these two cases. Case 4 compared with Case 5 then gives a measure of the attenuation due to the nozzle and guide pipe for a source on the insulation. Cases 7 and 8 were included to give the same information but for a source in water. In this case, however, the attenuation due to the guide pipe was determined from the more accurate DOT calculations in Section 5. Cases 10 and 11 were included to determine the contribution from a uniform contamination on the nozzle and guide pipe. Case 9 determines the dose rate from a localized heavier layer of contamination over a 6-inch long section of the guide pipe. Case 12 was added to confirm that a heavier layer on the wall similar to that on the guide pipe in Case 9 would add very little.

#### 4.1. Case 1 -- Source in Ring on Wall

The model for Case 1 is shown in Figure 8. The geometry and dimensions were obtained from Figures 3 and 4. The source for this case is the "bathtub ring" near the top of the cavity wall. Reference 6 on page 3.2-4 states that "present interpretation considers the bathtub ring to extend from the upper edge of the wall coating (approximately 5'-6" above the (basement) floor level) to the maximum level of accident water flooding (approximately 8'-6" above floor level)." This corresponds to from 7'-0" (213.36 cm) to 10'-0" (304.80 cm) above the cavity floor since the cavity floor is 1'-6" below the basement floor. The M-7 path of detector locations starts at the reference plane tangent to the bottom of the reactor vessel (see Figure 3) at an elevation of 290'-5-7/16" (288.13 cm above the cavity floor). Detector locations were selected every 6 inches along the M-7 path to 162 inches withdrawn from the reference plane. The distance withdrawn and corresponding z coordinate are listed in Table 2. While a contamination level of 242.93  $\mu\text{Ci}/\text{cm}^2$  was used in QADMOD, 220  $\mu\text{Ci}/\text{cm}^2$  will be used for the comparison with measurements. The initial source in QADMOD was 220  $\mu\text{Ci}/\text{cm}^2$  but due to a correction in the conversion of Ci to the number of gammas per second, the QADMOD results are equivalent to 242.93  $\mu\text{Ci}/\text{cm}^2$  with the correction. This value is consistent with the value quoted for painted surfaces within the elevation range of the bathtub ring. The results from QADMOD for Case 1 were multiplied by 0.906 to correct for the source strength (220/242.93) and by 0.84 in the nozzle region and 0.83 in the guide pipe region to account for the nozzle and guide pipe attenuation (see results for Cases 4 and 5 below). The results are tabulated in Table 2 and plotted in Figure 9.

#### 4.2. Case 2 -- Source on Wall Below Ring

The QADMOD model for Case 2 is similar to that for Case 1 except the source is on the wall below the ring (Region 2 in Figure 8). A source level of 55.21  $\mu\text{Ci}/\text{cm}^2$  was used in the QADMOD calculation for Case 2 and 50.0  $\mu\text{Ci}/\text{cm}^2$  will be used for comparison with measurements. This value is consistent with the value for painted walls in Reference 7. The results for Case 2 were multiplied by 0.906 to correct for source strength (50.0/55.21) and by 0.83 to account for attenuation in nozzle and guide pipe. The results are listed in Table 2 and plotted in Figure 9.

#### 4.3. Cases 3, 4, and 5 -- Source on Insulation

The QADMOD model for Case 3 is similar to the model for Case 1 shown in Figure 8 except the source is located in a disk 172 cm in radius extending from 281 cm to 289 cm above the cavity floor. This source is intended to represent the  $^{137}\text{Cs}$  contamination on the mirror insulation across the bottom of the reactor vessel with perhaps some contribution from the bottom of the reactor vessel. It is known that this part of the insulation was submerged when the water was at its highest level. Although in most cases steel surfaces have been observed to have less contamination than concrete (page 2.2-1, Reference 6), it seems highly probable that the mirror insulation under the vessel would have considerable contamination. The contamination in the water was approximately 137  $\mu\text{Ci}/\text{cm}^3$  at the time the water receded from the insulation (pages 4 and 9, Reference 8) and its elevation is within the range of the bathtub ring (page 3.2-4, Reference 6). The mirror insulation has multiple horizontal surfaces and, in general, horizontal surfaces are more contaminated than are vertical surfaces (page 2.2-1, Reference 6). For example, particulate matter has been observed on top of overhead cables and supports (page 23, Reference 8). A contamination of 244.8  $\mu\text{Ci}/\text{cm}^2$  was used in QADMOD, however, only 80  $\mu\text{Ci}/\text{cm}^2$  will be used for the comparison with measurements. The results for Case 3 were multiplied by 0.327 to correct for the source strength (80/244.8) and by 0.84 in the nozzle region and 0.83 in the guide pipe region to account for attenuation in these materials (see results for Cases 4 and 5).

Cases 4 and 5 are variations of Case 3. The gamma source was the same but the detector locations were changed to be along the vertical axis and a simulation of a nozzle and guide pipe were added coaxially to the detector points in Case 4. Case 5 is similar but with the nozzle and guide pipe removed. A comparison of Cases 4 and 5 then indicates the attenuation of gammas originating on the insulation due to the nozzle or guide pipe. Dose rates from Cases 4 and 5 are listed in Table 3 at various heights on the axis. The results indicate an attenuation factor

of about 0.84 in the nozzle region and 0.83 in the guide pipe region.

#### 4.4. Cases 6, 7, and 8 -- Source in Water

The model for QADMOD Case 6 is similar to that for Case 1 (Figure 8) except the source is located in the water. The contamination in the water was  $5.5 \mu\text{Ci}/\text{cm}^3$  in December, of 1986 (page 2.2-2, Reference 6). A source of  $4.897 \mu\text{Ci}/\text{cm}^3$  was used in QADMOD, however,  $2.16 \mu\text{Ci}/\text{cm}^3$  will be used for the comparison with measurements. The attenuation of the gammas originating in the water by the guide pipe and incore assembly was obtained from the DOT calculations in Section 5. A factor of 0.643 was observed. Case 6 QADMOD results were not used below the water. Some of the source points used in QADMOD were too close to detector locations. The QADMOD results under water were replaced with those from standard formulas for a semi-infinite medium. The results for both Case 6 and the hand calculated values were multiplied by 0.441 to correct for source strength ( $2.16/4.897$ ) and by 0.643 for attenuation in the guide pipe. The results are listed in Table 2 and are plotted in Figure 9.

The results for Cases 7 and 8 were replaced with the more accurate DOT calculations in Section 5.

#### 4.5. Case 9 -- Localized Source on Guide Pipe

QADMOD Case 9 was included to study the effect of a localized source on the guide pipe. A  $^{137}\text{Cs}$  source of  $100 \mu\text{Ci}/\text{cm}^2$  was located over a 6-inch length of the surface of an essentially infinitely long guide pipe. The DOT calculations in Section 5 show that the shift in gamma spectrum and increased sensitivity of the detector as the water is approached does not explain the peak observed at the air/water interface. The cause of the peak is more likely due to a localized source that may have been built up over time on the surface of the guide pipes just above the water level. The water level has fluctuated a number of times since the level has been near 2 feet in the cavity. Each time the water level has increased and then returned to the 2-foot level, a section of the guide pipe (6 inches for a 4-inch change in water level) would have been left wet. As the water evaporated, some of the  $^{137}\text{Cs}$  may have been left on the surface. If during the next increase in water level some of the  $^{137}\text{Cs}$  did not dissolve, then there would be a tendency for the contamination to buildup with each cycle. For the comparison with measurements, the localized contamination was assumed to be  $220 \mu\text{Ci}/\text{cm}^2$ . (A value of  $100 \mu\text{Ci}/\text{cm}^2$  was used in QADMOD.) That is, the contamination was made the same as that on a painted wall within the elevation range of the bathtub ring. The results are listed in Table 4 and are plotted in Figure 10.

4.6. Cases 10 and 11 -- Uniform Source  
on Nozzle and Guide Pipe

Cases 10 and 11 were added to consider uniform contamination on the guide pipe and nozzle. Source levels of  $111.29 \mu\text{Ci}/\text{cm}^2$  were used in the calculations. Values selected for use in the comparison with measurements were  $5 \mu\text{Ci}/\text{cm}^2$  below the elevation of the ring and  $20 \mu\text{Ci}/\text{cm}^2$  over the elevation range of the ring. As stated earlier, QADMOD results are proportional to the source strength used. Therefore, even large changes, as were made in this case, can be accommodated by multiplying by a constant. The results are listed in Table 2 and plotted in Figure 9.

4.7. Case 12 -- 4-Inch High Ring  
Source on Wall

The final QADMOD calculation, Case 12, considered a 4-inch high ring of  $^{137}\text{Cs}$  on the concrete wall just above the water level. This calculation was made to confirm that a ring on the concrete over the same height as the localized source on the guide pipe and with a strength of  $220 \mu\text{Ci}/\text{cm}^2$  would only contribute a very small amount to the M-7 traverse.

## 5. TRANSPORT CALCULATIONS

One-dimensional ANISN and two-dimensional DOT transport calculations were employed to investigate the observed peak in detector current near the air/water interface in the M-7 traverse (see Figure 5). It has been postulated that the peak might be due to gammas originating above the water and scattering back from the water at a lower energy. Since the sensitivity of the detector increases as the energy decreases, a higher current could be expected as the ion chamber approaches the water surface. The ANISN and DOT calculations are documented in Reference 9.

Both the ANISN and DOT calculations used the  $P_3$  Legendre polynomial scattering approximation and  $S_8$  quadrature (48 scattering angles) and the CASK 23-E cross section library with 40 energy groups. Only the last 18 of these are used for gammas. The  $^{137}\text{Ba}$  gamma falls into energy group 34.

The first part of this task was to generate a response table for the miniature ion chamber current; that is, to determine a constant for each energy group such that the product of that constant and the gamma flux for the group yields the ion chamber current for that energy group. A similar table for dose rate was already available in the cross section library. Information available on which the current response table could be based included the theoretical variation with energy of the Compton scattering and photoelectric cross sections for xenon (gas in ion chamber) and the measured calibration constant in air and in water described in Section 3. An ANISN model was developed representing each of the two measured configurations. A trial response table based on the theoretical cross section was used initially. The table was then iteratively adjusted until the calculated ratio of current-to-dose rate matched the measured ratio for both the in air and in water cases.

The DOT model of the cavity beneath the reactor vessel is shown in Figure 11. An RZ cylindrical geometry was used. The R coordinate is along the horizontal direction in Figure 11 and the z coordinate is the vertical direction. The axis of the cylinder is along the z direction at the left of the figure. There is symmetry in the  $\phi$  direction. Two DOT calculations were made. In one, the source was in a disk at the top simulating the mirror insulation and had a strength of  $200 \mu\text{Ci}/\text{cm}^2$ . In the other, the source was  $4.4 \mu\text{Ci}/\text{cm}^2$  of  $^{137}\text{Cs}$  dissolved in the 2 feet of water at the bottom of the cavity (Zone 2 in Figure 11). The calculated ion chamber current is plotted in Figure 12 for the insulation source and in Figure 13 for the source in water. In both cases the current is plotted for the ion chamber inside and outside the guide pipe. The ratio of the two gives a measure of the attenuation due to the guide pipe.

The phenomena of scattered gammas increasing the detector current can be observed in the traverse outside the guide tube in Figure 12. The size of the peak, however, does not match that observed (see Figure 5). Also, the peak is greatly reduced inside the guide tube and, therefore, there is even more difference between the observed peak in Figure 5 and the peak due to the shift in gamma spectrum.

The DOT calculation with the source in the water provides a measure of the ion chamber sensitivity for this configuration. The ion chamber currents and dose rates are listed in Table 5 for several points inside and outside the guide tube. The ratios yield a sensitivity of  $5.49 \times 10^{-13}$  amp/R/hr inside the guide tube under the water and  $14.8 \times 10^{-13}$  amp/R/hr outside the guide tube in the water. Also, Table 5 indicates an attenuation factor of 0.643 on the dose rate due to the guide tube.

## 6. RESULTS

The QADMOD results for the M-7 traverse are tabulated in Tables 2 and 4 and are plotted in Figures 9 and 10. The total dose rate obtained using the selected source strengths is compared with the measured profile in Figure 1. The agreement is sufficiently good to conclude that the M-7 measured traverse can be matched with calculations using only cesium contamination sources.

Ion chamber current measurements for the M-9 traverse are plotted in Figure 7. The current is approximately constant from 104 to about 190 inches withdrawn from the reference plane. The calculated values for the M-7 traverse should also apply to the M-9 traverse over the range of 104 to 165 inches withdrawn. The M-9 current averages  $0.022 \times 10^{-10}$  amp in this range. Dividing by the sensitivity value calculated by DOT in Section 5 gives a measured dose rate of 4.0 R/hr. Comparing this with the calculated dose rate in Figure 1 shows that the calculated value is approximately equal to the average of the measured dose rates of about 2.5 R/hr for M-7 and 4 R/hr for M-9 in the range of 105 to 165 inches withdrawn. The measured current for the M-9 traverse increases considerably from 190 to 232 inches withdrawn. Contamination on surfaces in the back grouted wall area would be expected to make the radiation level increase as the 232-inch position is approached. The observed current is within the range that could be expected particularly if there are unpainted concrete surfaces or surfaces with damaged paint. The peak and dip in the curve could be caused by either hangers or other supports providing extra localized shielding or perhaps in some way a localized source close to the guide pipe.

## 7. REFERENCES

1. R. Rainisch, TMI-2 Technical Bulletin, Gamma Scanning of the Cavity Under the Reactor Vessel, May 2, 1986; B&W Records Center No. 38-1013553-00.
2. Letter from W. R. Cobean, Jr. to F. R. Standerfer, "QAD Study, TMI-2 Under Vessel Dose Rates," January 7, 1987, with Burns & Roe calculations; B&W Records Center No. 38-1013558-00.
3. Letter from R. Rainisch to G. R. Eidam, "Analysis of the M-7 Gamma Profile in the Lower Reactor Vessel Cavity," February 3, 1987; B&W Records Center No. 38-1013554-00.
4. TMI-2 Technical Planning Department, June 1985, Data Report on Analysis of Gamma Scanning of In-Core Detector #18 (L-11) in Lower Reactor Vessel Head. TPO/TMI-175, Rev. 0, Middletown, PA, GPU Nuclear Corporation; B&W Records Center No. 38-1013559-00.
5. 32-1167934-00, "QADMOD Calculations of Dose Rate Beneath TMI-2 Reactor Vessel."
6. TMI-2 Technical Planning Department, February 1987, Data Report on Reactor Building Radiological Characterization. TPO/TMI-125, Rev. 1, Middletown, PA, GPU Nuclear Corporation. See 32-1167934-00, Appendix A, for copy of pages referred to in this report.
7. GPU Nuclear Letter of June 2, 1986 from C. H. Distenfeld to G. R. Eidam, "Comparison of Measured and Calculated Exposure Rates in Two Selected RB Basement Locations," 4550-86-0196; B&W Records Center No. 38-1013555-00.
8. Thomas E. Cox, et al., Reactor Building Basement Radionuclide and Source Distribution Studies, GEND-INF-011, Vol III, June 1983; B&W Records Center No. 38-1013556-00.
9. 32-1167926-00, "ANISN and DOT Calculations of Dose Rate Beneath TMI-2 Reactor Vessel."

Table 1. List of QADMOD Cases

Case No.	Source	Guide Tube Present?	Detector Locations
1	Ring on wall, 242.93 $\mu\text{Ci}/\text{cm}^2$	No	Along withdrawal path for M-7
2	Wall other than ring, 55.21 $\mu\text{Ci}/\text{cm}^2$	No	Along withdrawal path for M-7
3	Insulation, 244.8 $\mu\text{Ci}/\text{cm}^2$	No	Along withdrawal path for M-7
4	Insulation, 244.8 $\mu\text{Ci}/\text{cm}^2$	Yes	Along vertical path
5	Insulation, 244.8 $\mu\text{Ci}/\text{cm}^2$	No	Along vertical path
6	Water, 4.897 $\mu\text{Ci}/\text{cm}^3$	No	Along withdrawal path for M-7
7	Water, 4.897 $\mu\text{Ci}/\text{cm}^3$	Yes	Along vertical path
8	Water, 4.897 $\mu\text{Ci}/\text{cm}^3$	No	Along vertical path
9	6" length on vertical pipe, 100.0 $\mu\text{Ci}/\text{cm}^2$	Yes	Along vertical path
10	Uniform contamination on nozzle, 111.29 $\mu\text{Ci}/\text{cm}^2$	Yes	Along vertical path
11	Uniform contamination on pipe, 111.29 $\mu\text{Ci}/\text{cm}^2$	Yes	Along vertical path
12	4" high ring on wall just above water level	No	Along withdrawal path for M-7

Table 2. Calculated Dose Rate Along M-7 Withdrawal Path

Distance Withdrawn, inches	z, cm	Ring	Wall	Insulation	Water	On <sup>1</sup> Nozzle or Pipe	Total R/hr
		220 $\mu\text{Ci}/\text{cm}^2$ R/hr	50 $\mu\text{Ci}/\text{cm}^2$ R/hr	80 $\mu\text{Ci}/\text{cm}^2$ R/hr	2.16 $\mu\text{Ci}/\text{cm}^3$ R/hr	R/hr	
0	288.13	2.23	0.50	5.11	0.24	1.06	9.14
6	272.89	2.28	0.54	3.97	0.26	1.06	8.11
12	257.65	2.27	0.58	2.73	0.28	1.13	6.99
18	242.41	2.25	0.63	2.09	0.31	1.13	6.41
24	227.17	2.19	0.67	1.66	0.34	0.28	5.14
30	211.93	2.10	0.71	1.36	0.38	0.28	4.83
36	196.76	1.99	0.75	1.14	0.42	0.28	4.58
42	181.73	1.87	0.77	0.97	0.47	0.28	4.36
48	166.96	1.74	0.79	0.84	0.53	0.28	4.18
54	152.54	1.62	0.79	0.73	0.60	0.28	4.02
60	138.55	1.50	0.79	0.65	0.67	0.28	3.89
66	125.09	1.39	0.77	0.58	0.75	0.28	3.77
72	112.24	1.30	0.76	0.52	0.83	0.28	3.69
78	100.09	1.22	0.74	0.48	0.91	0.28	3.63
84	88.71	1.15	0.72	0.44	0.99	0.28	3.58
90	78.17	1.08	0.70	0.40	1.07	0.28	3.53 <sup>2</sup>
96	68.56	1.03	0.69	0.37	1.12	0.28	3.49 <sup>2</sup>
102	59.91	1.04	0.71	0.37	1.49	0.00	3.61 <sup>2</sup>
108	52.30	0.97	0.42	0.35	2.13	0.00	3.87
114	45.76	0.72	0.25	0.28	2.28	0.00	3.53
120	40.35	0.53	0.17	0.21	2.33	0.00	3.24
126	36.09	0.40	0.14	0.16	2.40	0.00	3.10
132	33.01	0.33	0.12	0.13	2.40	0.00	2.98
138	31.14	0.29	0.13	0.11	2.40	0.00	2.93
144	30.48	0.27	0.14	0.10	2.40	0.00	2.91
150	30.48	0.27	0.18	0.09	2.40	0.00	2.94
156	30.48	0.26	0.21	0.09	2.40	0.00	2.96
162	30.48	0.25	0.23	0.08	2.40	0.00	2.96

<sup>1</sup>20  $\mu\text{Ci}/\text{cm}^2$  in region of ring, 5  $\mu\text{Ci}/\text{cm}^2$  below ring, 0  $\mu\text{Ci}/\text{cm}^2$  in water.

<sup>2</sup>See Table 4 for addition due to localized source.

Table 3. Attenuation in Nozzle and Guide  
Pipe From QADMOD

Receiver No.	Z, cm	Region	Case 4 With Nozzle, Guide Pipe and Incore R/hr	Case 5 Without Nozzle Guide Pipe or Incore R/hr	Ratio Case 4-to- Case 5
1	288.13	Nozzle	18.7	22.7	0.82
2	272.89	Nozzle	13.5	15.7	0.86
3	257.65	Guide Pipe	9.31	10.6	0.88
4	242.41	Guide Pipe	7.07	8.14	0.87
5	227.17	Guide Pipe	5.62	6.53	0.86
6	196.69	Guide Pipe	3.79	4.48	0.85
7	166.21	Guide Pipe	2.68	3.24	0.83
8	135.73	Guide Pipe	1.96	2.42	0.81
9	105.25	Guide Pipe	1.48	1.87	0.79
10	74.77	Guide Pipe	1.13	1.48	0.76

Table 4. Dose Rate From Localized Source  
on Guide Pipe

Distance Withdrawn From Ref Plane, inches	Distance Relative to Peak, inches	Dose Rate From 220 $\mu$ Ci/cm <sup>2</sup> Over a 6" Length, R/hr
93.99	-5.01	0.31
94.83	-4.17	0.99
95.66	-3.34	4.20
96.50	-2.50	9.04
97.75	-1.25	11.95
98.17	-0.83	12.10
98.58	-0.42	12.17
99.00	0.00	12.19
99.42	0.42	12.17
99.83	0.83	12.10
100.25	1.25	11.95
101.50	2.50	9.04
102.34	3.34	4.20
103.17	4.17	0.99
104.01	5.01	0.31

Table 5. Ion Chamber Sensitivity and Guide Pipe Attenuation From DOT Results<sup>1</sup>

J	Calculated Dose Rate			Calculated Current	
	Inside Guide Pipe I=1 R/hr	Outside Guide Pipe I=17 R/hr	Attenuation Factor	Inside Guide Pipe I=1 amp	Outside Guide Pipe I=17 amp
6	4.17	6.45	0.647	$2.26 \times 10^{-12}$	$9.26 \times 10^{-12}$
7	4.30	6.69	0.643	$2.37 \times 10^{-12}$	$9.91 \times 10^{-12}$
8	4.34	6.77	0.641	$2.40 \times 10^{-12}$	$10.13 \times 10^{-12}$
9	4.30	6.70	<u>0.642</u>	$2.37 \times 10^{-12}$	$9.95 \times 10^{-12}$
			Avg = 0.643		

J	Sensitivity	
	I=1 amp/R/hr	I=17 amp/R/hr
6	$5.42 \times 10^{-13}$	$14.4 \times 10^{-13}$
7	$5.51 \times 10^{-13}$	$14.8 \times 10^{-13}$
8	$5.53 \times 10^{-13}$	$15.0 \times 10^{-13}$
9	<u><math>5.51 \times 10^{-13}</math></u>	<u><math>14.9 \times 10^{-13}</math></u>
Avg = $5.49 \times 10^{-13}$		$14.8 \times 10^{-13}$

<sup>1</sup>From DOT case with source in water.

FIGURE 1. CALCULATED AND MEASURED DOSE RATE, M-7 TRAVERSE

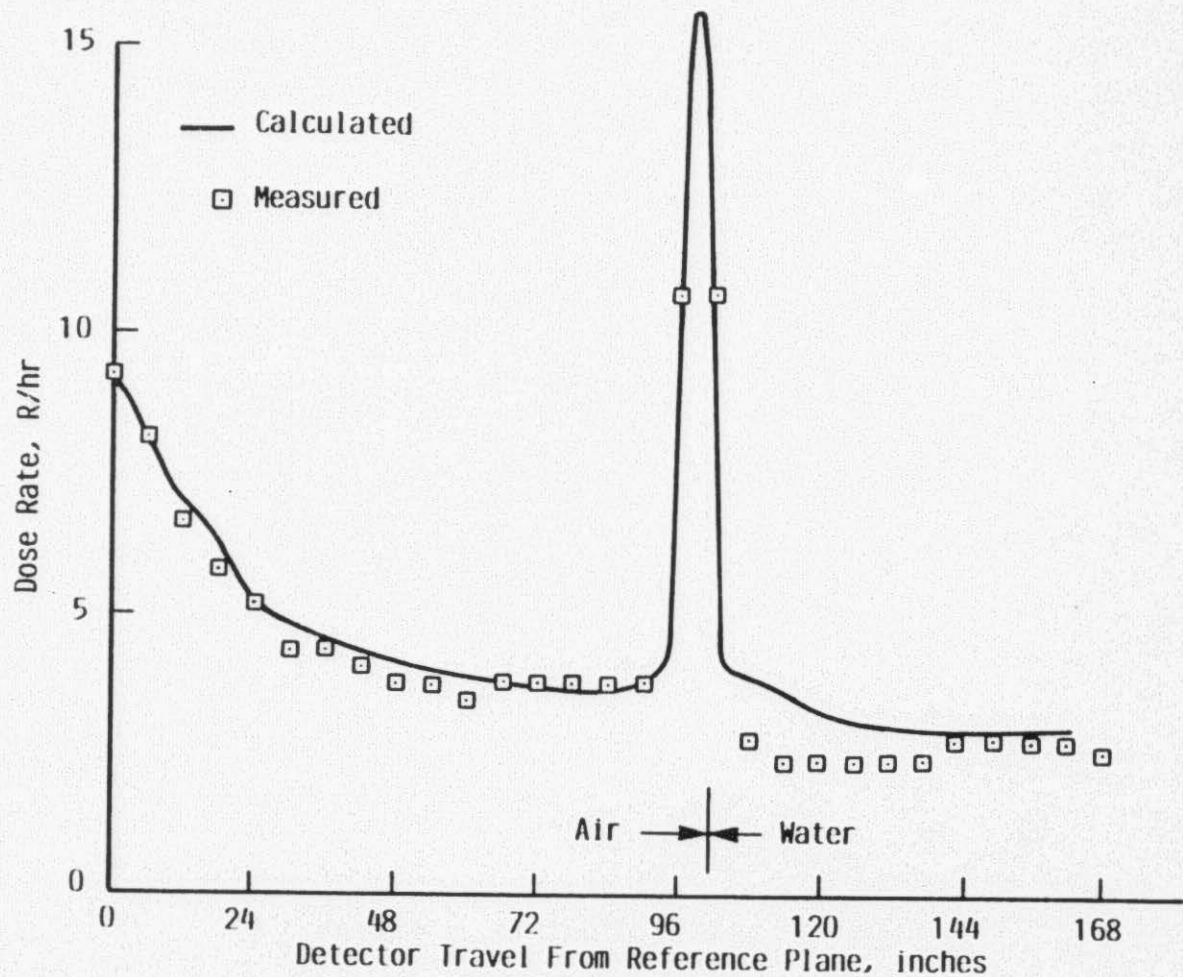
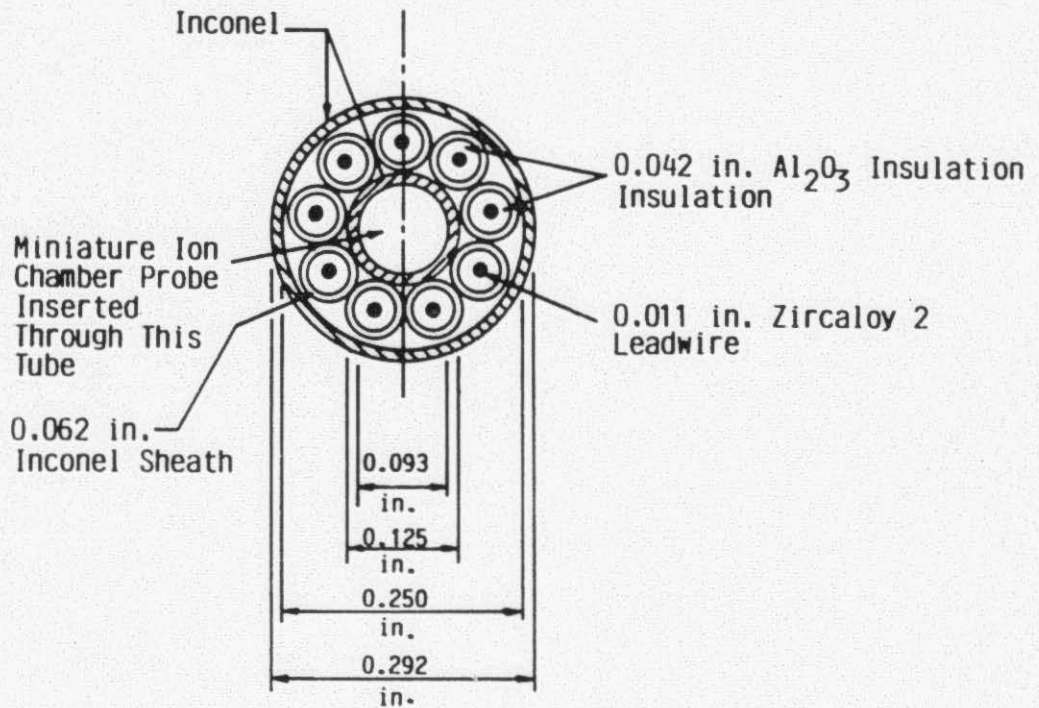


FIGURE 2. IN-CORE DETECTOR CROSS SECTION



(Assembly Includes Seven Neutron-Sensitive Detectors, One Background Detector, and One Thermocouple)

FIGURE 3. PRIMARY SHIELD CAVITY UNDER REACTOR VESSEL,  
ELEVATION VIEW (FROM FIG. 2 REF 1)

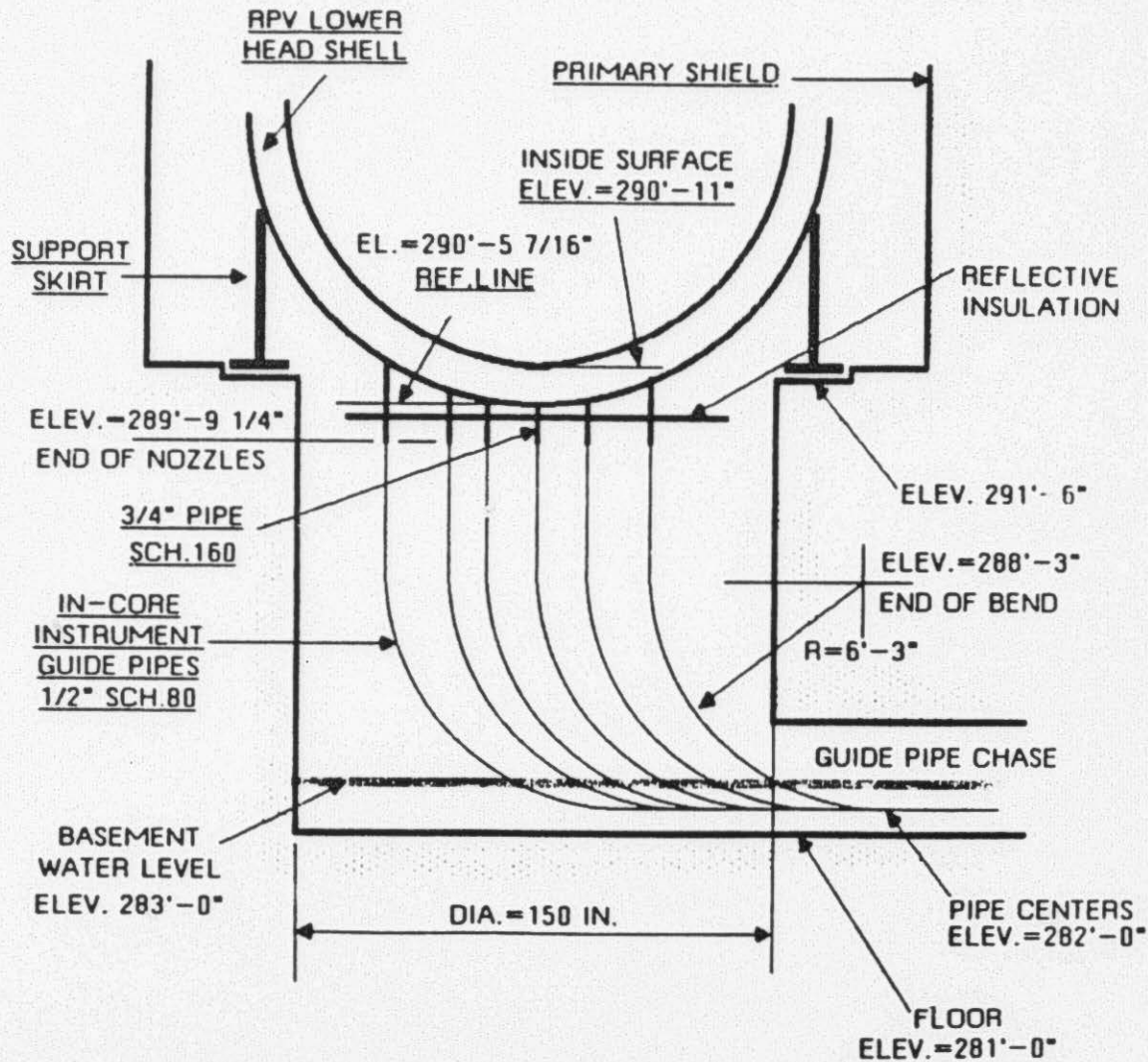


FIGURE 4. PATH OF IN-CORE GUIDE PIPE #13 (M-7)  
(FROM FIG. 4 REF 1)

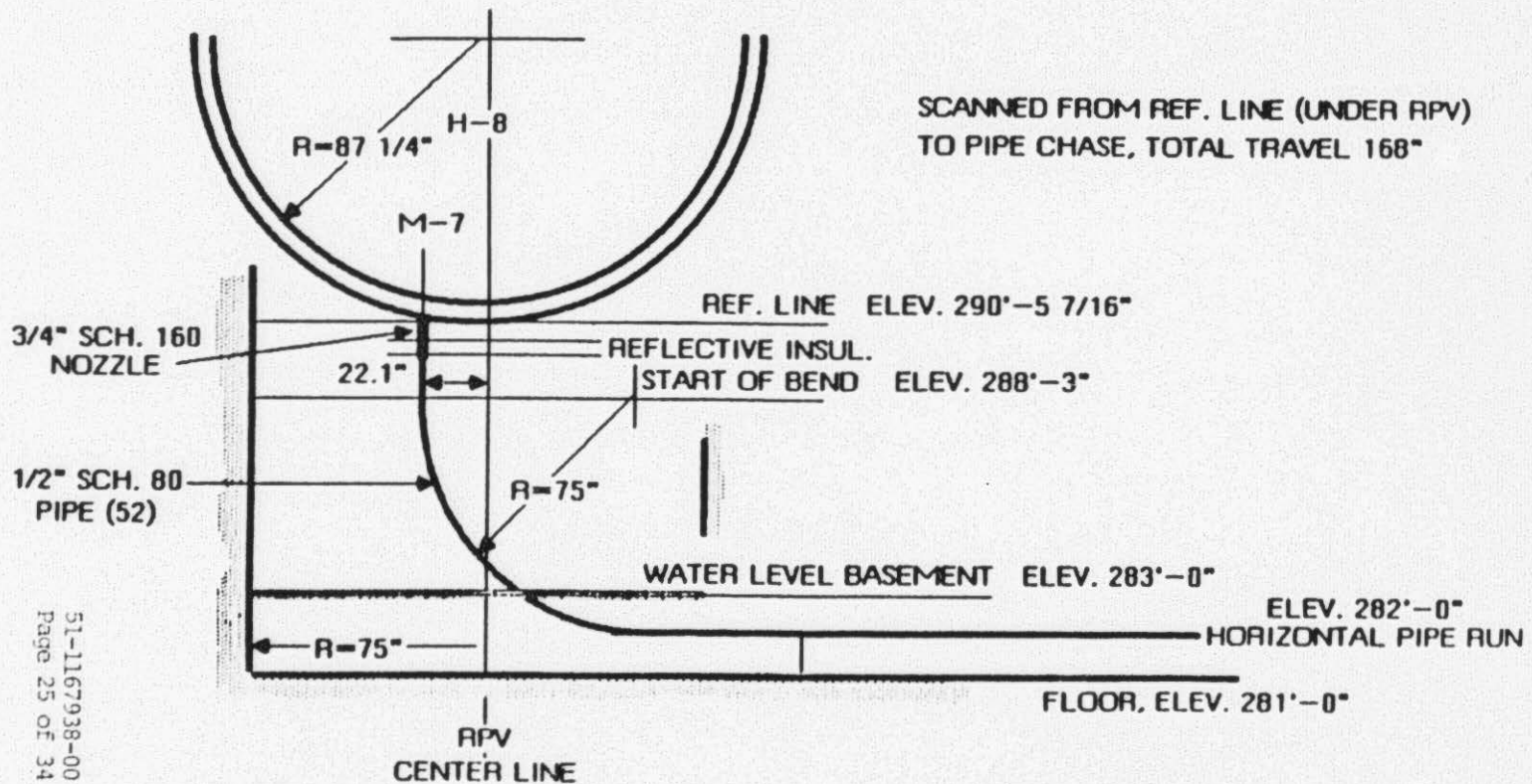


FIGURE 5. CURRENT PROFILE MEASURED AT LOCATION M-7  
(FROM FIG. 5 REF 1)

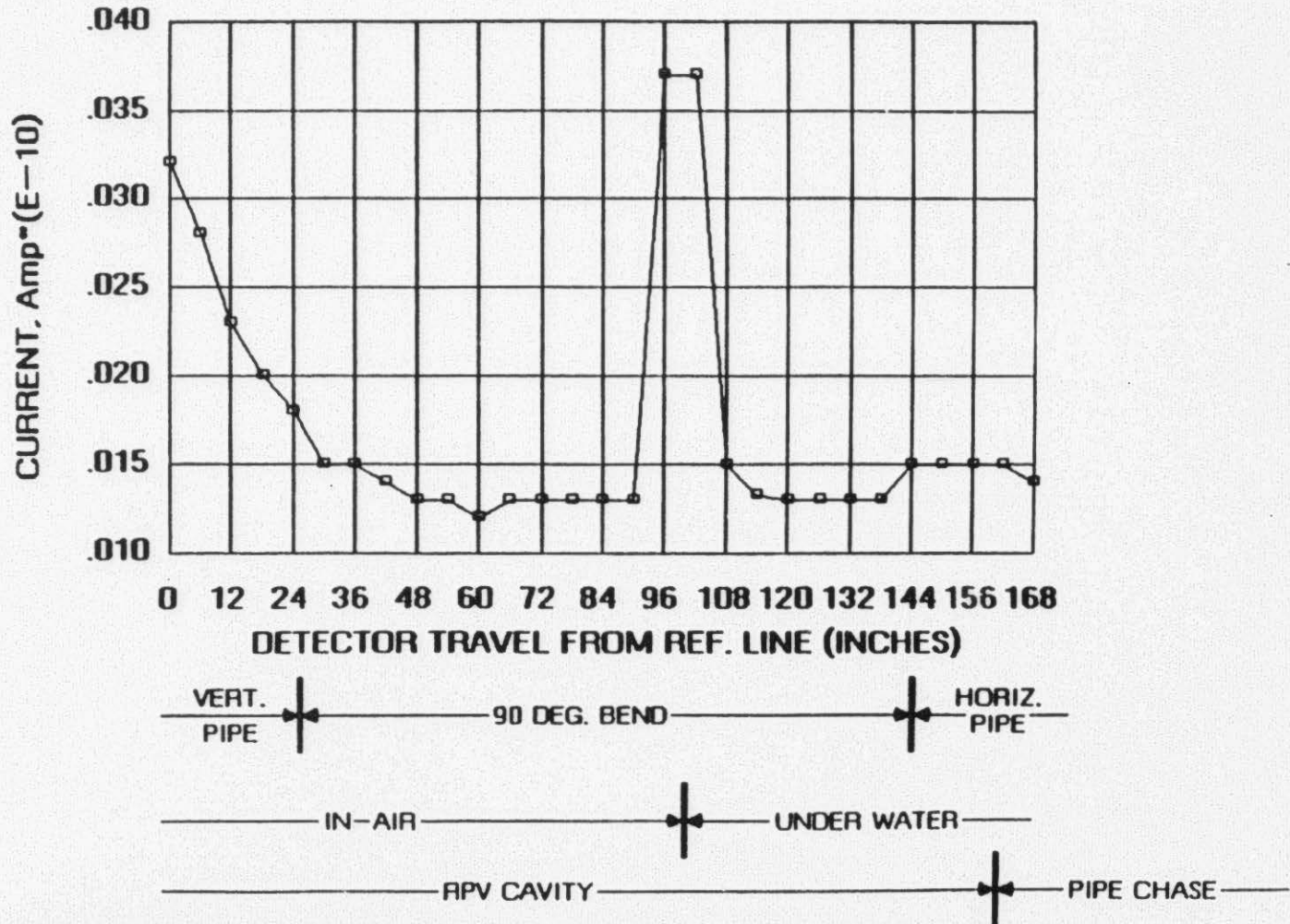


FIGURE 6. PATH OF IN-CORE GUIDE PIPE #16 (M-9)  
(FROM FIG. 6 REF 1)

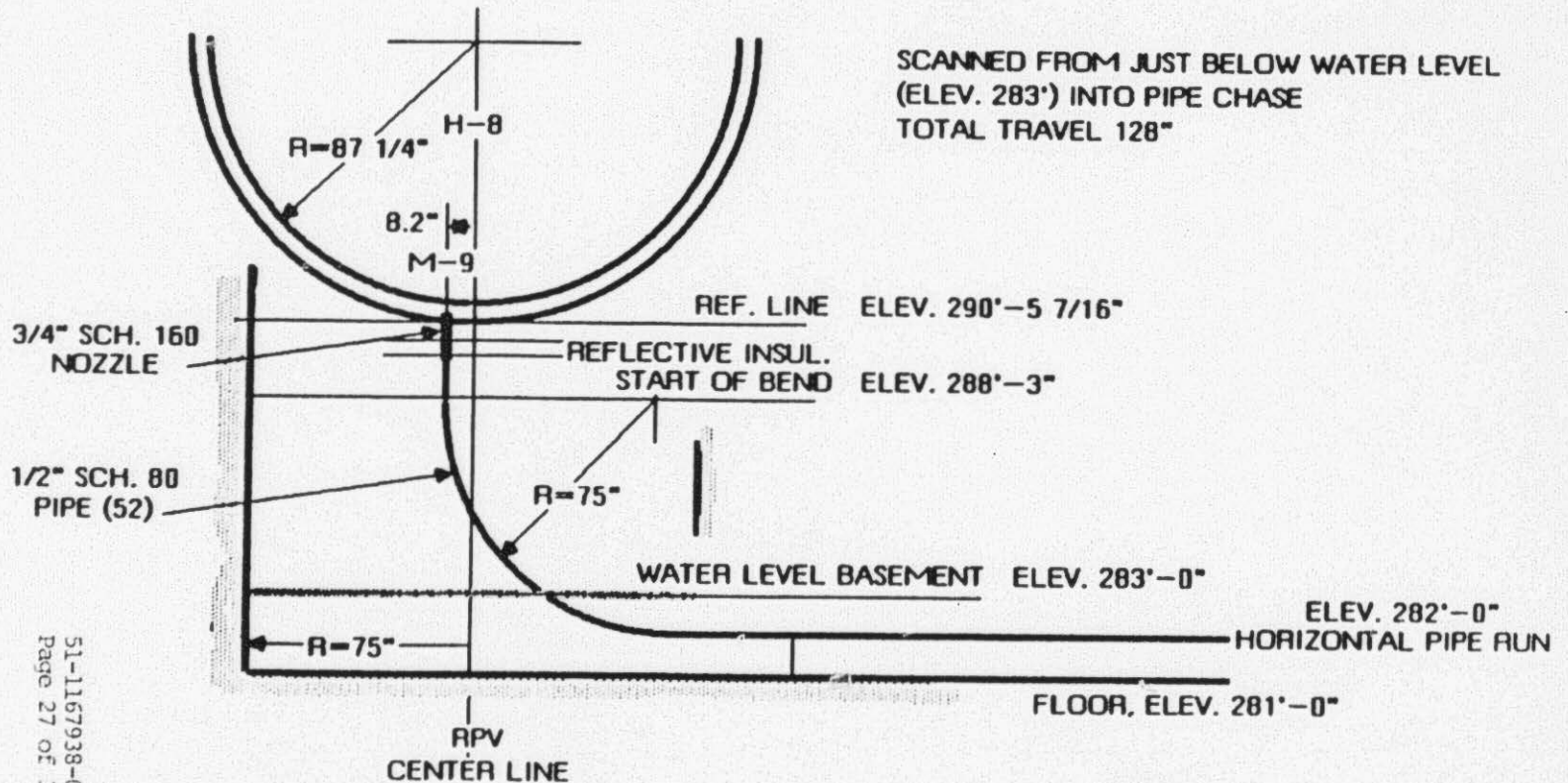


FIGURE 7. (CURRENT PROFILE MEASURED AT LOCATION M-9  
(FROM FIG. 7 REF 1))

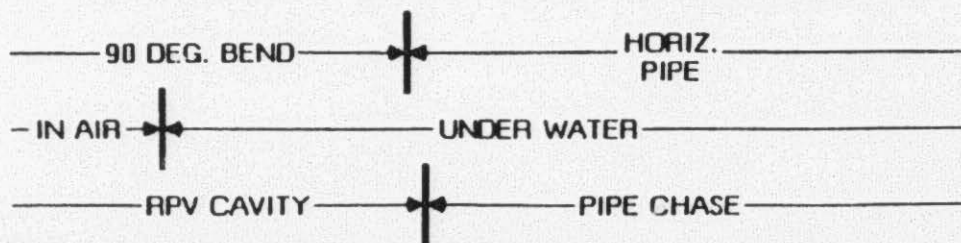
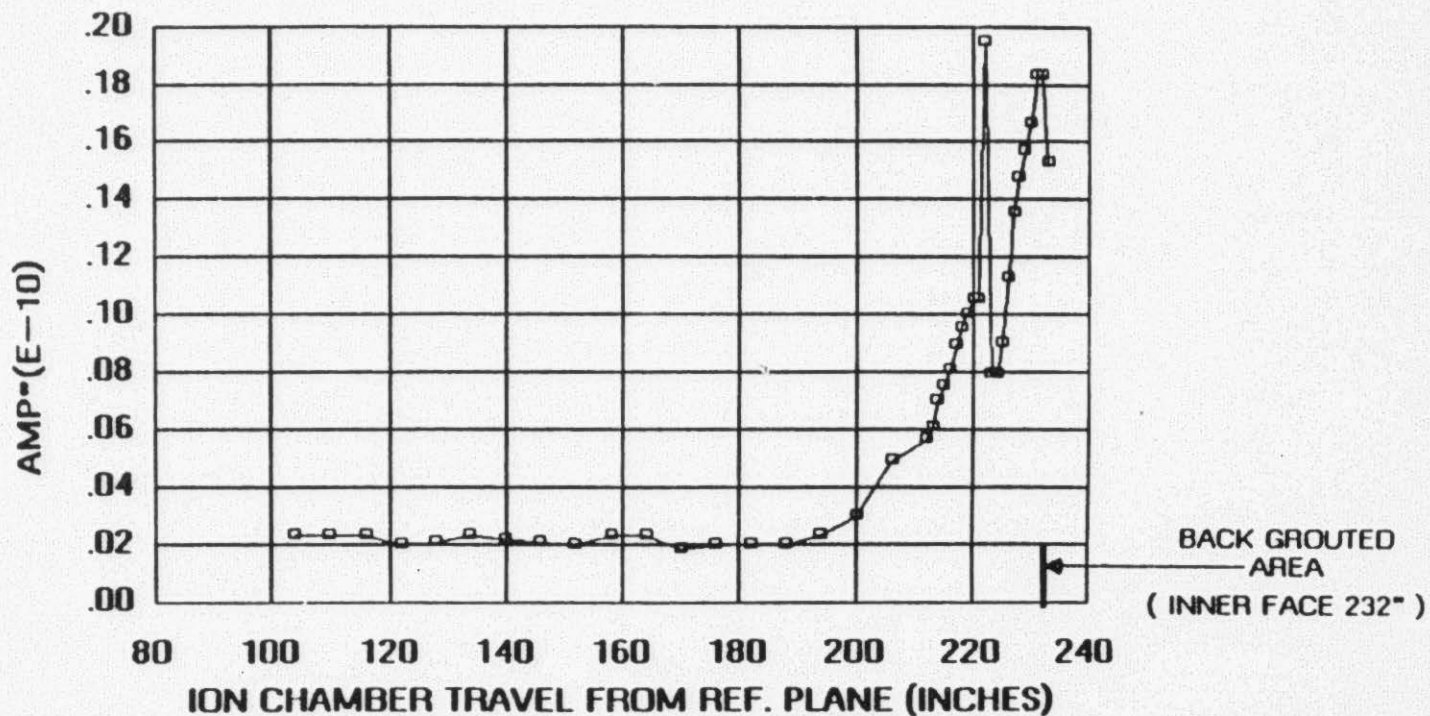
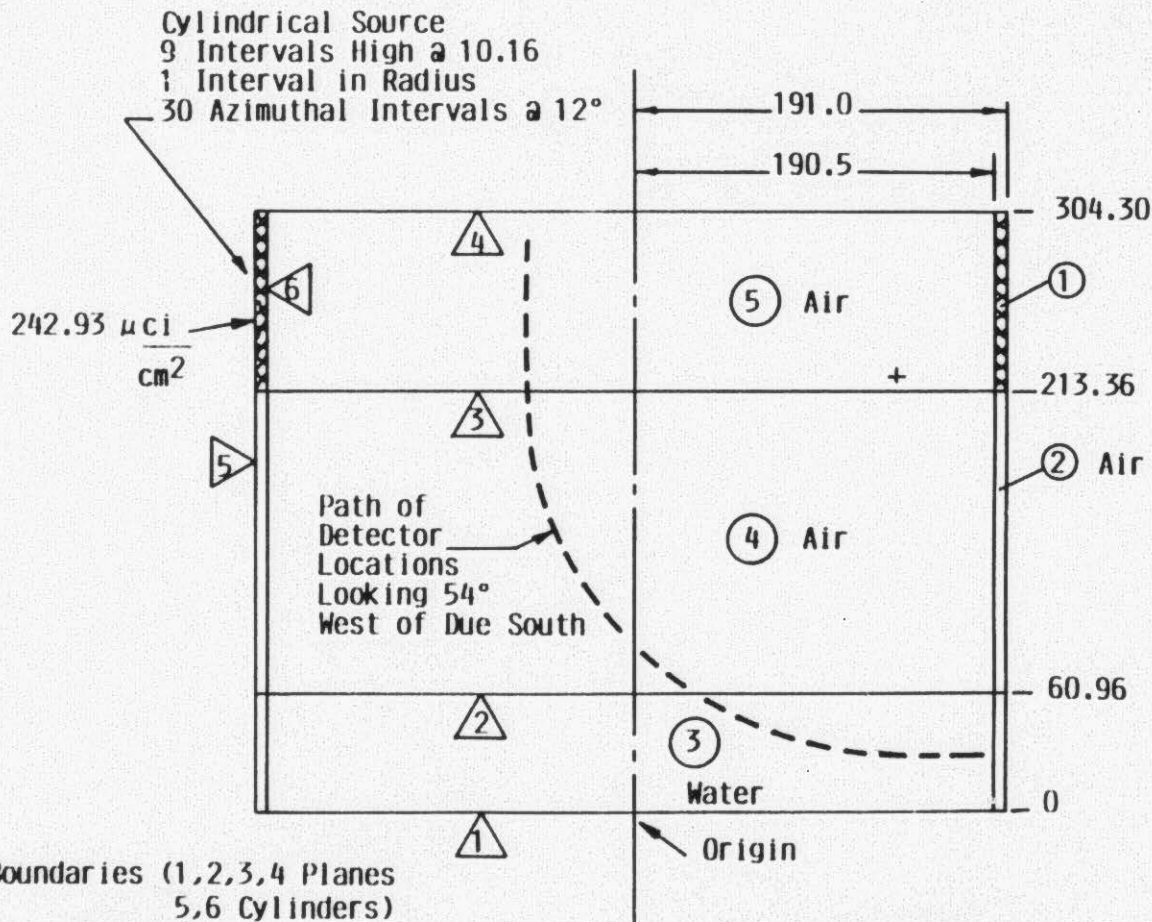


FIGURE 8. QADMOD MODEL FOR CASE 1, RING SOURCE



△ Boundaries (1,2,3,4 Planes  
 5,6 Cylinders)

○ Region Numbers

All Dimensions in cm

FIGURE 9. DOSE RATE FROM VARIOUS SOURCES, M-7 TRAVERSE

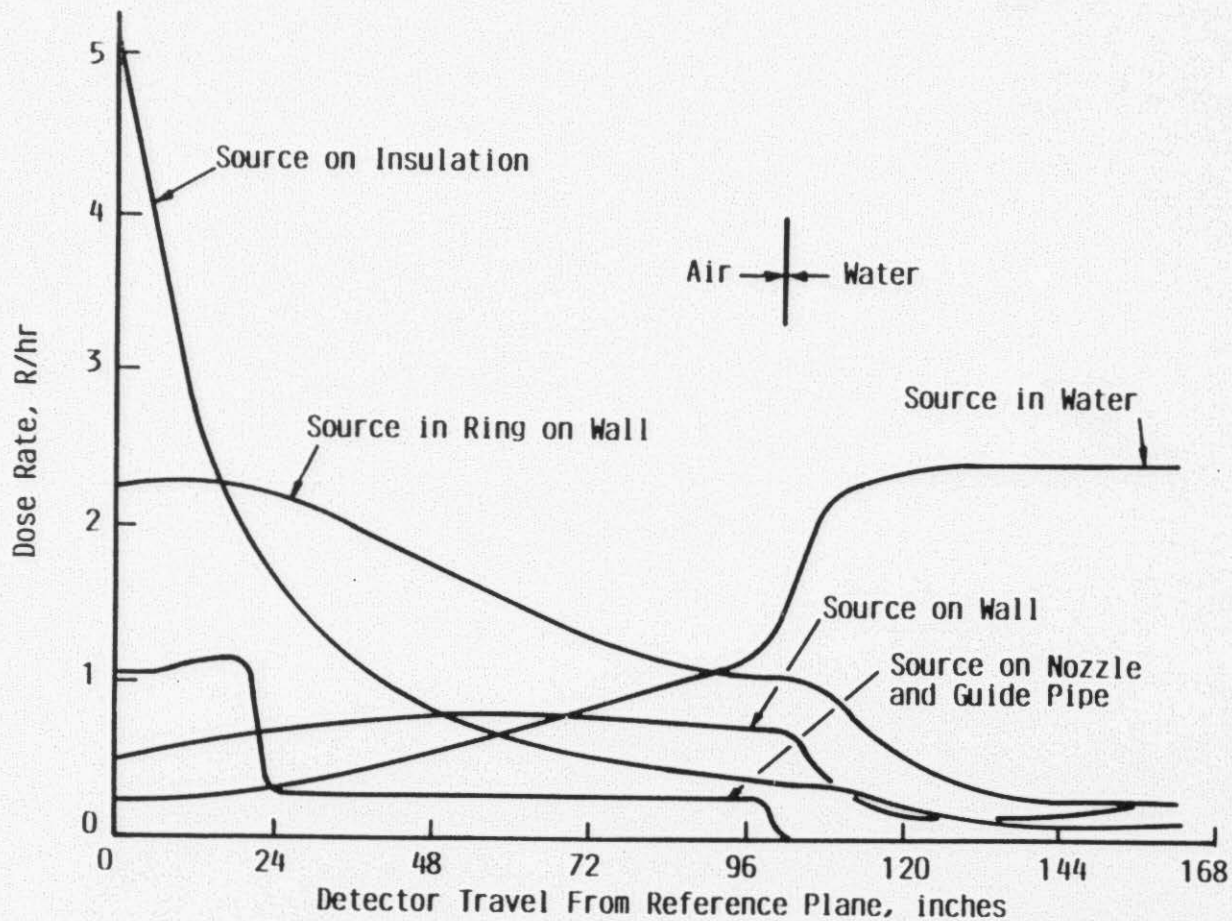


FIGURE 10. DOSE RATE FROM LOCALIZED SOURCE ON GUIDE PIPE

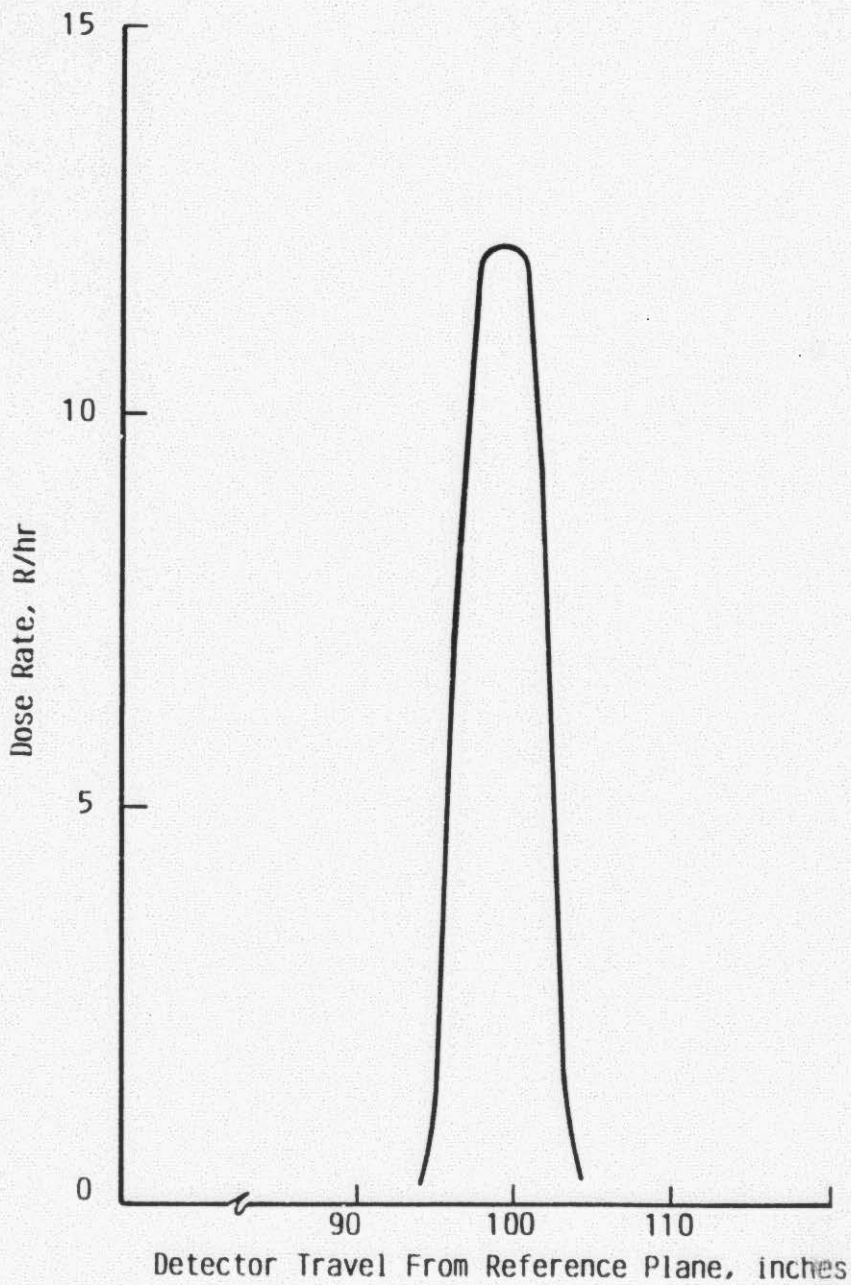
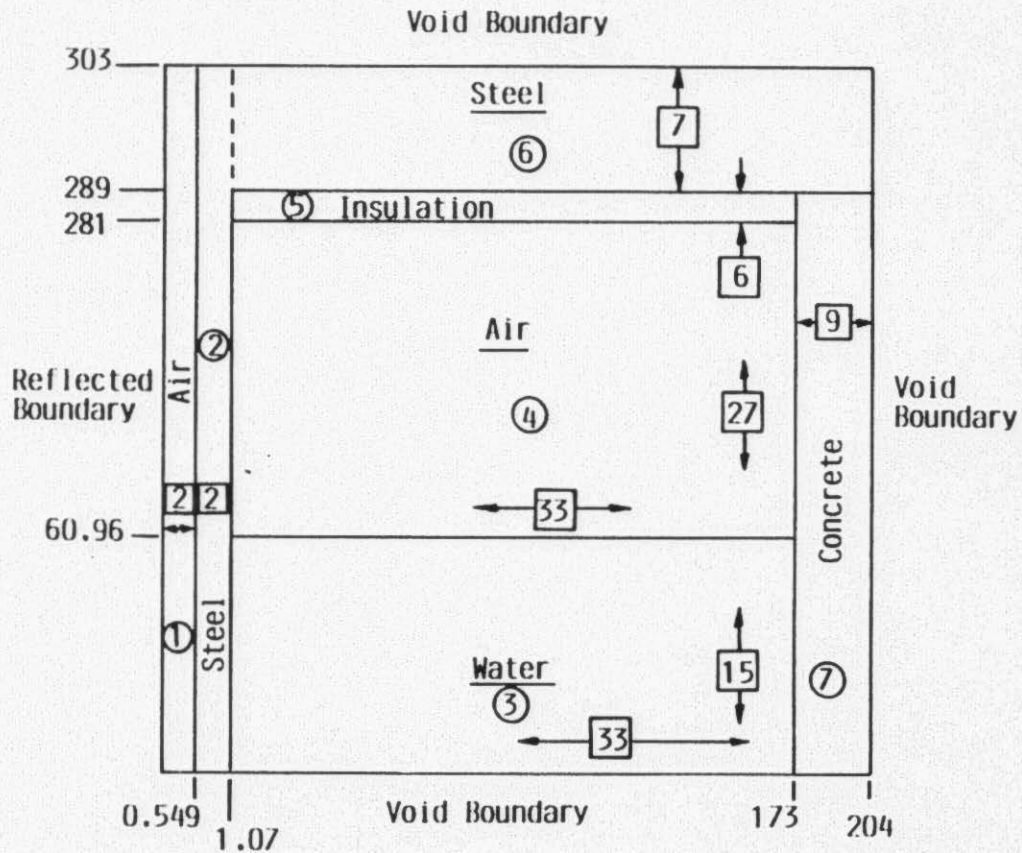


FIGURE 11. DOT MODEL



  $\Rightarrow$  Zone n  
  $\Rightarrow$  m Intervals

Dimensions in cm

FIGURE 12. DETECTOR CURRENT DUE TO INSULATION SOURCE

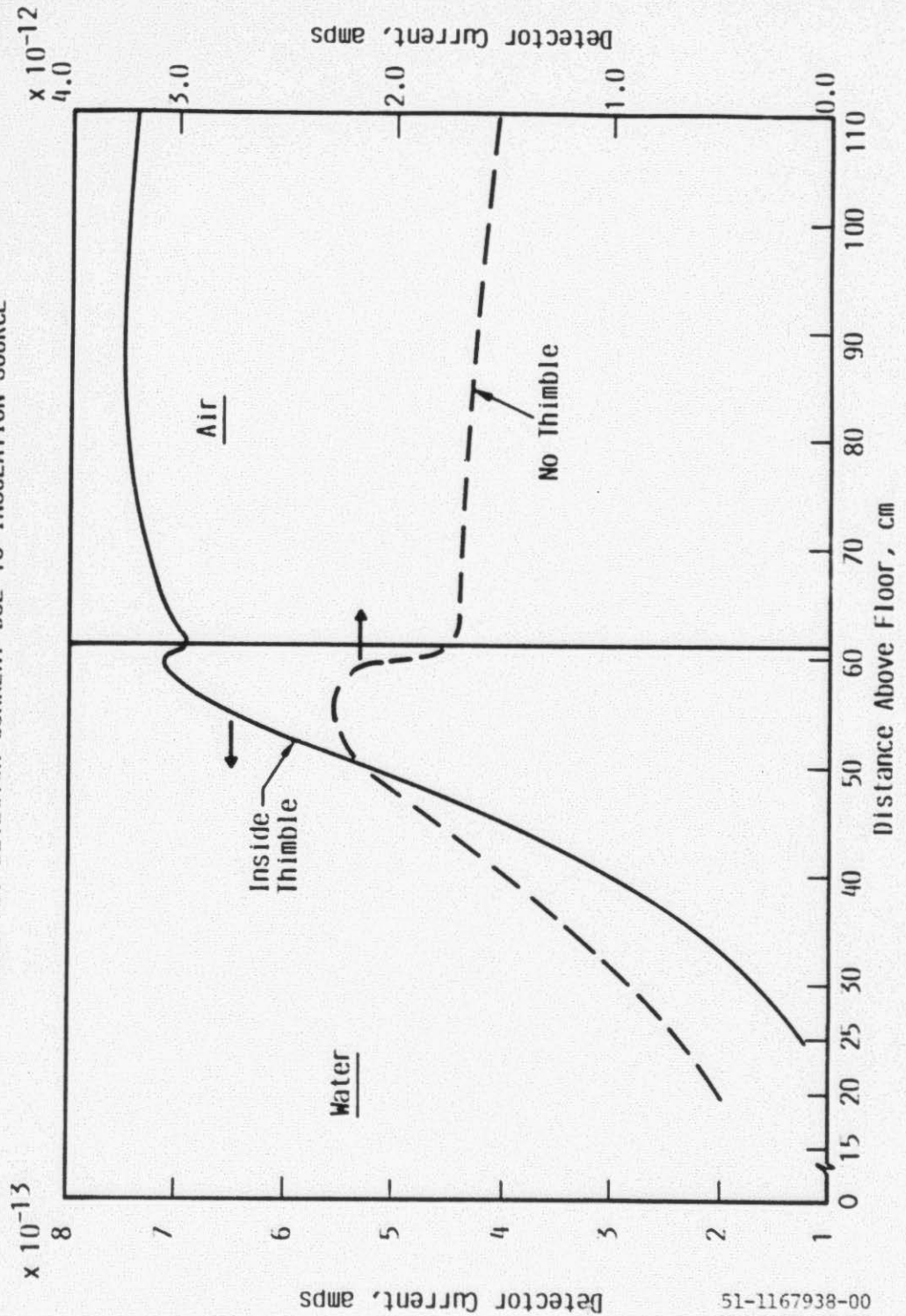


FIGURE 13. DETECTOR CURRENT DUE TO SOURCE IN WATER

